Qubit addressing using hyperfine-interaction control by an electric field in a magnetic crystal

Myeonghun Song* and Soonchil Lee
Department of Physics, Korea Advanced Institute of Science and Technology, Daejeon 305-701, Republic of Korea

David J. Lockwood
Institute for Microstructural Sciences, National Research Council, Ottawa, Ontario K1A 0R6, Canada
(Received 7 May 2010; published 13 July 2010)

We demonstrate experimentally the hyperfine-interaction control by an electric field, which is the operating principle of the addressable qubit operation in a silicon-based solid-state quantum computer in a new quantum computer system, a magnetic crystal. The transferred hyperfine field at a F^- nucleus caused by neighboring Mn^{2+} electron spins in an antiferromagnetic MnF_2 single crystal was measured by ^{19}F nuclear magnetic resonance (NMR) with an external electric field applied along the [110] crystal direction. The electric field splits the ^{19}F NMR peak into two resolved lines that come from the F nuclei located at geometrically equivalent sites. A line splitting of 56 kHz was achieved at an electric field of 3.4 V/μm. One of the F^- nuclear spins could be flipped selectively by a composite radio-frequency pulse while leaving the other unchanged, thereby demonstrating qubit addressing via electric field control of the hyperfine interaction.

DOI: 10.1103/PhysRevA.82.012311 PACS number(s): 03.67.Lx, 75.50.Ee, 76.60.−k

The silicon-based nuclear spin quantum computer proposed by Kane [1] is one of the most attractive quantum computer architectures because of its smart design and ready implementation using current silicon technology. The building blocks of Kane's model have been experimentally demonstrated; these include control of the hyperfine interaction by an electric field [2], readout of electron [3] and nuclear [4] spin states, and long-lived quantum memory [5]. The hyperfine interaction plays a key role in the logic operation and the measurement of a quantum bit (qubit) in the model. The gate operation is performed by using the magnetic resonance technique. The hyperfine interaction is controlled by an external electric field, making the resonance frequency of a selected qubit different from that of others so that each qubit can be addressed independently. The hyperfine field control by the electric field is also used for the so-called controlled-NOT operation, which is the coupled qubit operation that is essential for a quantum system to be a quantum computer.

Kane's model uses the nuclear spins of phosphorus ions embedded in a silicon crystal in regular spacing as qubits. The system should be operated at very low temperature and high magnetic field to suppress the fluctuations of electron spins that would generate a hyperfine field. This difficult constraint on the experimental conditions can be eased somewhat if a quantum system can be used where the electron spins are naturally fixed. A magnetic crystal is an example belonging to this case. In this work, we present an experimental demonstration of qubit addressing using hyperfine field control by an electric field in a magnetic crystal. It is known that the hyperfine field of fluorine nuclei changes linearly with applied electric field in antiferromagnetic MnF_2 [6,7]. Therefore, the nuclear spins of the fluorine ions in the ordered state of a MnF_2 crystal can work as qubits that can be selectively operated by nuclear magnetic resonance (NMR). NMR has been applied to the experimental realization of a quantum computer with successful results [8–10]. Most of the NMR quantum information processors were implemented with molecules in a liquid state. A few models were proposed that used crystals, but experimental realization was never achieved [11,12]. The external electric field changes the transferred hyperfine field of F^- nuclei due to Mn^{2+} electron spins and splits the ^{19}F NMR spectral peak into two peaks, which are independently addressable by rf pulses.

A plate-shaped sample with dimensions of 6.0 × 6.5 × 0.66 mm^3 was cut from a single crystal of MnF_2. Silver epoxy electrodes were coated on both sides of the large surfaces in order to apply an external electric field of up to 3.4 V/μm along the [110] direction. An rf coil was wound around the sample to apply a rotating magnetic field in the direction perpendicular to the [001] direction. The sample was mounted inside a closed-cycle cryostat that can lower the temperature down to 6.3 K. An external magnetic field of 53 mT was applied along the [001] direction to split the zero-field NMR spectrum into two well-separated peaks. A pulsed NMR method was adopted to measure the hyperfine field and control the nuclear spins of the F^- ions.

In MnF_2, the magnetic moments of Mn ions are antiferromagnetically ordered along the c axis (Fig. 1). Fluorine ions are nonmagnetic but transferred hyperfine fields are generated at the position of each fluorine nucleus by its three neighboring Mn ion spins. The external magnetic field B_0 pointing along the c-axis direction is either parallel or antiparallel to the hyperfine field at the F^- site, depending on the direction of the neighboring Mn spins. Since the external field is much weaker than the hyperfine field, the total field is stronger and weaker than the hyperfine field at the F ions marked by H and L in Fig. 1, respectively. A B_0 of 53 mT shifted the resonance frequency of the F^- nuclear spin at the H site (L site) by 2.1 MHz (−2.1 MHz) from its zero-field resonance frequency of 159.93 MHz at 6.3 K. The external electric field pointing along the [110] direction pulls the F^- ions at the H site along the same direction, making one half of them move closer (H_1) to the neighboring Mn^{2+} ion with spin down and the other half farther (H_2). This increases and decreases the hyperfine fields of the F nuclei at the H_2 and H_1 sites and therefore further splits the NMR spectrum coming from the

*hunmsong@kaist.ac.kr

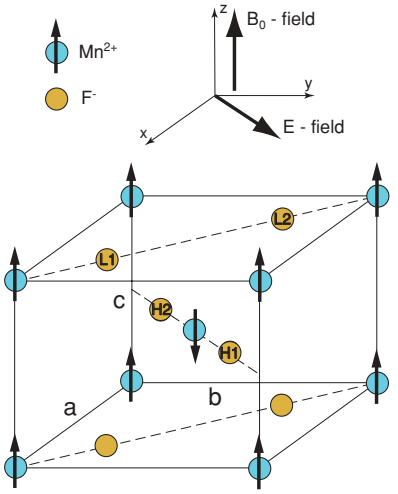

FIG. 1. (Color online) Crystal structure of tetragonal ($a = b \neq c$) MnF_2 and the configuration of the applied electric field, applied magnetic field, and Mn^{2+} spin orientation.

F^- nuclei at the H site, which was already separated from the L peak by the magnetic field. Those at the L site are not affected by the electric field in the first-order approximation since the direction from the L sites to the neighboring Mn sites is orthogonal to the electric field direction [6].

Figures 2(a) and 2(b) show free-induction decay (FID) signals from the F^- nuclear spin at the H site after the 90° rf pulse with external dc voltages of 0 and 2250 V on the electrodes, respectively. The FID signal in Fig. 2(b) shows a beat indicating that there are two different resonance frequencies, while that in Fig. 2(a) shows only a single frequency component. The reference frequency was set 0.2 MHz off resonance on purpose to clearly observe the beat form, whereas all other data were taken on resonance. Figures 2(c) and 2(d) show the NMR spectra obtained by the Fourier transformation of the FID signals. The spectrum was a very well defined single Gaussian shape with a width of about 50 kHz. The low-frequency NMR spectrum of the two split lines that arises from the F^- nuclear spin at the L site is shown in Fig. 2(c). The electric field left the NMR spectrum unaltered except for a small shift. However, the electric field splits the high-frequency peak coming from the F^- nuclear spin at the H site, as shown in Fig. 2(d). The splitting of the NMR spectrum increases as the electric field increases. This clearly shows that the hyperfine field from Mn^{2+} electron spins is controllable by the external electric field since the NMR frequency is proportional to the hyperfine field. The variation of the hyperfine field with the electric field is because of (i) the variation of the interionic distance, (ii) the covalency between Mn^{2+} and F^- ions, and (iii) the variation of s-p hybridization of $2s$ and $2p$ orbitals of F^- ions [6]. The maximal line splitting of 56 kHz was achieved in an electric field of 3.4 V/μm. This result is consistent with the previous data taken by continuous-wave NMR experiments [7,13].

Now, we move to the gate operation on nuclear spins and demonstrate the qubit addressing in the single-qubit operations in the way proposed by Kane's model. Since the line splitting of 56 kHz was comparable to the line broadening, each nuclear spin could not be selectively operated by a single

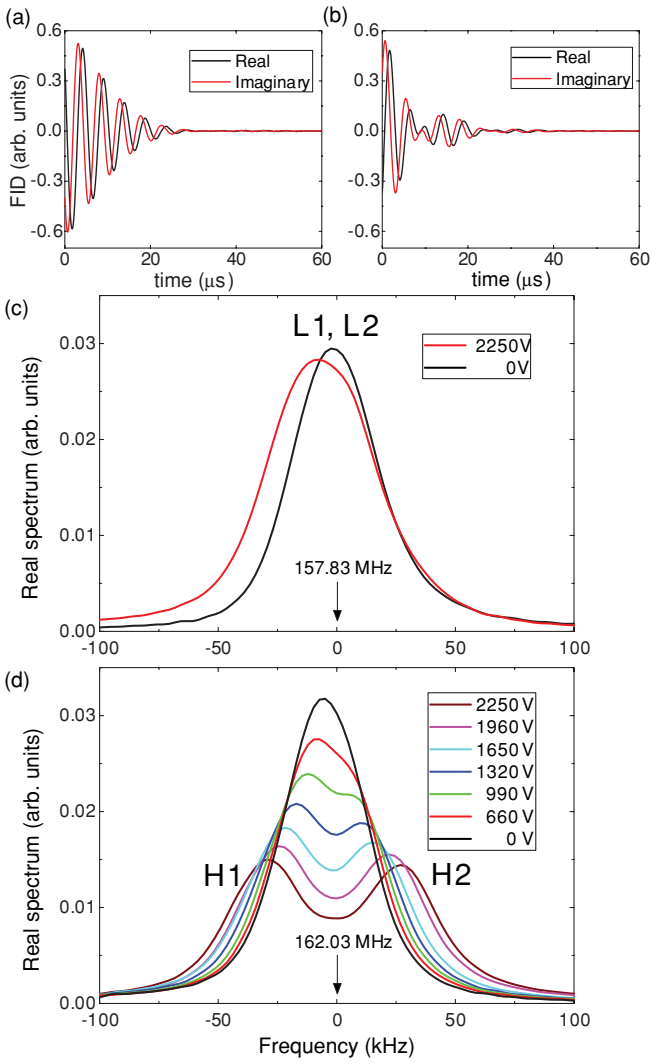

FIG. 2. (Color online) FID signal from the F^- nuclear spin at the H site after the 90° rf pulse with an external dc voltage of (a) 0 V and (b) 2250 V. (c) Low-frequency NMR peaks coming from the F^- nuclear spin at the L site with and without the external electric field. The spectra were obtained by the Fourier transformation of the FID signals. (d) High-frequency NMR peaks coming from the F^- nuclear spin at the H site for various electric fields. The legend correlates with the curves whose peaks go from the lowest (top curve) to the highest (bottom curve) electric field.

pulse. Instead, a composite pulse sequence, which has been extensively studied after the first demonstration of the NMR quantum information processor [14], was adopted to achieve selective inversion corresponding to the NOT operation in quantum information logic. By a composite pulse sequence

$$R^{H_1}_{x,\text{composite}}(\pi) = R^{H_1,H_2}_{-y}\left(\frac{\pi}{2}\right) D\left(\frac{\pi}{2}\right) R^{H_1,H_2}_{x}\left(\frac{\pi}{2}\right), \qquad (1)$$

the nuclear spin at the H_1 site is inverted while that at the H_2 site is unchanged. In Eq. (1), $R^{H_1,H_2}_{\alpha}(\theta)$ is a rotation operator that rotates nuclear spins at the H_1 and H_2 sites around the α axis simultaneously by the angle θ. This operation is implemented by a hard pulse in the NMR technique. $D(\theta)$ is a free time-evolution operator implemented by a time delay

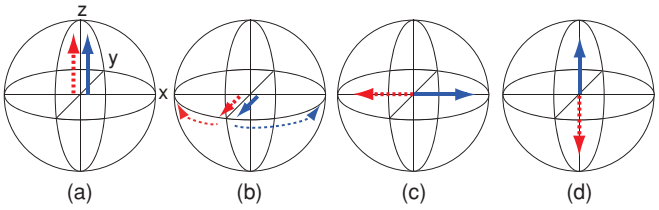

FIG. 3. (Color online) Evolution of the two nuclear spins at the H_1 and H_2 sites by the composite pulse sequence in Eq. (1) visualized in the Bloch sphere. (a) Initial state of the nuclear spins. The red dashed (blue solid) arrow represents the F^- nuclear spin at the H_1 site (H_2 site). (b) After a 90° hard pulse along the x direction, both nuclear spins point in the $-y$ direction. (c) After a free time evolution of 8.9 μs, two nuclear spins rotate in opposite directions by 90°. (d) Final state after a 90° hard pulse along the $-y$ direction. The nuclear spin at the H_1 site is selectively inverted.

t_θ between rf pulses. During the time delay, the nuclear spins at the H_1 and H_2 sites rotate by the angle $\pm\theta$ around the z axis in the rotating frame, respectively. Since the NMR line splitting is 56 kHz in our experiment, $t_{\frac{\pi}{2}}$ is 8.9 μs. In Fig. 3, the effect of the composite pulse sequence, Eq. (1), on each nuclear spin is visualized in the Bloch sphere. As a result of the first operation, $R_x^{H_1,H_2}(\frac{\pi}{2})$, both nuclear spins point in the $-y$ direction [Fig. 3(b)]. After the free time evolution $D(\frac{\pi}{2})$, the nuclear spin at the H_1 site (H_2 site) lies on the $-x$ axis ($+x$ axis) [Fig. 3(c)]. The last operation, $R_{-y}^{H_1,H_2}$, completes the selective inversion of the nuclear spin at the H_1 site while returning the nuclear spin at the H_2 site to the original state [Fig. 3(d)].

Since the z component of a nuclear moment is unobservable in the NMR experiment, an additional hard pulse is required to read out the final states of nuclear spins. If we take a hard pulse along the $+y$ direction, $R_y^{H_1,H_2}(\frac{\pi}{2})$, as a reading pulse, the resulting pulse sequence is reduced to the following simple form:

$$R_y^{H_1,H_2}\left(\frac{\pi}{2}\right)R_{x,\text{composite}}^{H_1}(\pi) = D\left(\frac{\pi}{2}\right)R_x^{H_1,H_2}\left(\frac{\pi}{2}\right). \qquad (2)$$

In Fig. 4 the NMR spectra obtained after the first and second operations of the reduced composite pulse sequence in Eq. (2) are shown. Figure 4(a) shows the real and imaginary parts of the spectrum obtained after the first operation, $R_x^{H_1,H_2}(\frac{\pi}{2})$. After a 90° hard pulse along the x axis, the nuclear spins lie on the $-y$ axis; therefore, both peaks from the nuclear spins at the H_1 and H_2 sites have negative signs in the imaginary spectrum. Figure 4(b) shows the real and imaginary parts of the spectrum obtained after the second operation. In the real spectrum, the sign of the peak from the nuclear spin at the H_1 site is negative, meaning that the nuclear spin is inverted, while the sign of the peak from the nuclear spin at the H_2 site is positive because that spin is not inverted. Thus, a NOT operation was successfully implemented on the nuclear spins pointing up at the H_1 site selectively, leaving the state of the spins at the H_2 site unchanged.

In summary, we demonstrated an addressable qubit operation in a new quantum computer system, a magnetic crystal. A NOT operation was performed on the fluorine nuclei in antiferromagnetic MnF_2 by pulsed NMR. The hyperfine field

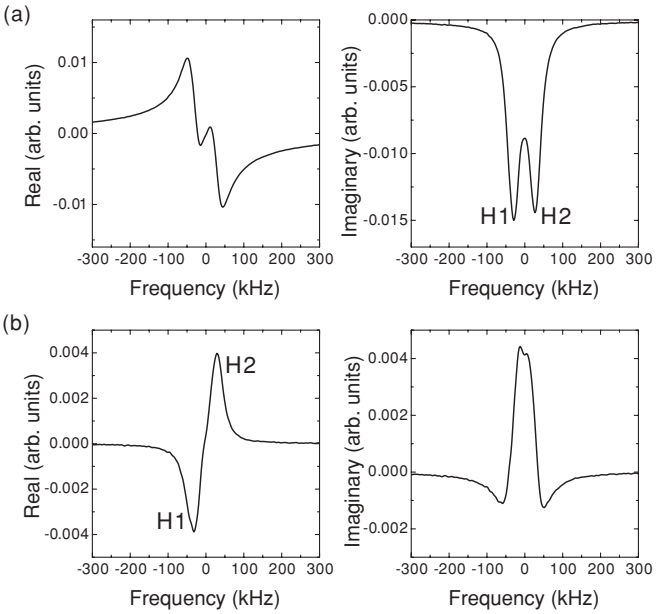

FIG. 4. NMR spectrum after each step of the reduced composite pulse sequence in Eq. (2). (a) Real and imaginary parts of the spectrum after the first operation, $R_x^{H_1,H_2}(\frac{\pi}{2})$. The signs of the peaks from the nuclear spins at the H_1 and H_2 sites are both negative in the imaginary part since both nuclear spins lie on the $-y$ axis. (b) Real and imaginary parts of the spectrum at the reading time. The sign of the peak from the nuclear spin at the H_1 site is negative while that from the H_2 site is positive. Only the nuclear spin at the H_1 site was selectively inverted.

was controlled by an external electric field as in Kane's model. The NMR spectrum was split into two peaks by the external magnetic field, one of which was split again by the electric field. This splitting created three independently addressable qubits in a unit cell. If the electric field direction was along the [100] direction, both of the lines split by the magnetic field could be split again by the electric field, making four addressable qubits. Each nuclear spin was successfully inverted by a composite pulse sequence. In a magnet, the indirect interaction via the spin wave is usually the main interaction among the nuclei of the magnetic ions. This Suhl-Nakamura interaction [15] would have some influence on nonmagnetic ions like fluorine in MnF_2, but it is likely that the indirect interaction between two fluorine nuclei would not be strong enough to be used for controlled qubit operations. Therefore, MnF_2 cannot be regarded as a real quantum computer system, but it is a good test bed to demonstrate qubit addressing by the electric field control of the hyperfine interaction. Coupled qubit operations by control of the interaction between the qubits remains for future study. It is another avenue to explore to justify more thoroughly the importance of the result for the field of quantum computing.

ACKNOWLEDGMENTS

We acknowledge Crystal Bank at Pusan National University, Korea, for providing the single crystal of MnF_2. This work was supported by the Korea Research Foundation Grant No. KRF-2008-313-c00290 and the Korea Science and Engineering Foundation Grant No. 2009-0078342.

[1] B. E. Kane, Nature **393**, 133 (1998).
[2] F. R. Bradbury, A. M. Tyryshkin, G. Sabouret, J. Bokor, T. Schenkel, and S. A. Lyon, Phys. Rev. Lett. **97**, 176404 (2006).
[3] R. Hanson, L. H. Willems van Beveren, I. T. Vink, J. M. Elzerman, W. J. M. Naber, F. H. L. Koppens, L. P. Kouwenhoven, and L. M. K. Vandersypen, Phys. Rev. Lett. **94**, 196802 (2005).
[4] A. Yang, M. Steger, D. Karaiskaj, M. L. W. Thewalt, M. Cardona, K. M. Itoh, H. Riemann, N. V. Abrosimov, M. F. Churbanov, A. V. Gusev, A. D. Bulanov, A. K. Kaliteevskii, O. N. Godisov, P. Becker, H.-J. Pohl, J. W. Ager, and E. E. Haller, Phys. Rev. Lett. **97**, 227401 (2006).
[5] J. J. L. Morton, A. M. Tyryshkin, R. M. Brown, S. Shankar, B. W. Lovett, A. Ardavan, T. Schenkel, E. E. Haller, J. W. Ager, and S. A. Lyon, Nature **455**, 1085 (2008).
[6] N. Bloembergen, Phys. Rev. Lett. **7**, 90 (1961).
[7] P. S. Pershan and N. Bloembergen, Phys. Rev. Lett. **7**, 165 (1961).
[8] N. A. Gershenfeld and I. L. Chuang, Science **275**, 350 (1997).
[9] D. G. Cory, A. F. Fahmy, and T. F. Havel, Proc. Natl. Acad. Sci. USA **94**, 1634 (1997).
[10] L. M. K. Vandersypen and I. L. Chuang, Rev. Mod. Phys. **76**, 1037 (2004).
[11] T. D. Ladd, J. R. Goldman, F. Yamaguchi, Y. Yamamoto, E. Abe, and K. M. Itoh, Phys. Rev. Lett. **89**, 017901 (2002).
[12] D. G. Cory, R. Laflamme, E. Knill, L. Viola, T. F. Havel, N. Boulant, G. Boutis, E. Fortunato, S. Lloyd, R. Martinez, C. Negrevergne, M. Pravia, Y. Sharf, G. Teklemariam, Y. S. Weinstein, and W. H. Zurek, e-print arXiv:quant-ph/0004104.
[13] P. S. Pershan, Phys. Rev. Lett. **7**, 280 (1961).
[14] J. Kim, J.-S. Lee, and S. Lee, Phys. Rev. A **61**, 032312 (2000).
[15] T. Nakamura, Prog. Theor. Phys. **20**, 542 (1958).